Intramolecular Excimer Kinetics of Fluorescent Dipyrenyl Lipids: 2. DOPE/DOPC Membranes

Kwan Hon Cheng,* Lucy Ruymgaart,* Lin-I Liu,* Pentti Somerharju,‡ and Istvan P. Sugar§

*Department of Physics, Texas Tech University, Lubbock, Texas 79409; ‡Department of Medical Chemistry, University of Helsinki, 00170 Helsinki, Finland; and §Departments of Biomathematical Sciences and Physiology & Biophysics, The Mount Sinai Medical Center, New York, New York 10029 USA

ABSTRACT The intramolecular dynamics of the excimer-forming dipyrenyl lipids ($Dipy_nPE$) of different chain lengths (n) in fully hydrated dioleoylphosphatidylethanolamine (DOPE) and dioleoylphosphatidyl-choline (DOPC) binary mixtures was investigated by the use of frequency-domain fluorescence intensity decay technique. Using a 3-state model (see companion paper), the extent of aggregation and rotational rate of the two covalently attached pyrene moieties in $Dipy_nPE$ were estimated from the frequency-domain data. At 1°C, the rotational rate and aggregation for $Dipy_4PE$ and $Dipy_{10}PE$ were insensitive to DOPE% of the lipid bilayer. At 27°C, the rotational rate decreased, whereas the aggregation increased steadily for $Dipy_{10}PE$ as the DOPE% of the bilayer increased from 0 to 80. However, an abrupt increase in the rotational rate and a decrease in the aggregation for $Dipy_{10}PE$ were detected as the DOPE% reached 100, at which point the membranes are in the inverted hexagonal (H_{II}) phase. No similar changes were found for $Dipy_4PE$. These results indicate that the presence of PE with large intrinsic-curvature increases the lateral stress at the region near the center of the bilayer, and that this stress can be relieved as the membranes enter the highly curved H_{II} phase.

INTRODUCTION

The self-assembly nature and polymorphic phase behavior of lipid/water mixtures have been a subject of extensive interest (Rand et al., 1990; Seddon, 1990; Gawrisch et al., 1992; Gruner, 1992; Lewis et al., 1994; Epand and Epand, 1994). In the familiar bilayer phase, such as lamellar liquid crystalline (L_α), the lipids are arranged in stacked bilayers with sheets of water between the polar surfaces of the lipid headgroups. On the other hand, in the nonbilayer inverted hexagonal (H_{II}) phase, the lipids are arranged in cylindrical tubes with their headgroups facing the long symmetric axes of the cylinders. The biological significance of several nonbilayer preferring lipids, e.g., unsaturated phosphatidylethanolamine (PE) (Cheng et al., 1986; Hui, 1993; Keller et al., 1993) and diacylglycerol (Cheng and Hui, 1986a), in native and reconstituted membranes, has been recognized for many years.

An interesting stress model (Seddon, 1990; Gawrisch et al., 1992) has been proposed on the mechanism of the formation of nonbilayer phases. According to this model, the lipid monolayer containing the nonbilayer phase preferring lipids has a characteristic nonzero spontaneous (or intrinsic) curvature, and confining this monolayer into a planar bilayer form results in the development of a hypothesized curvature-associated lateral stress in the lipid layer. Because of the presence of other competing free energy terms (Gruner, 1992), such as electrostatic, hydration, hydrocarbon packing, and others, the lipid monolayer in the presence of an opposite monolayer can retain the planar bilayer form, but at the expense of a high intrinsic curvature-related bending energy. A detailed understanding of this intrinsic curvature-related stress in membranes at the molecular level is required.

Spectroscopy is a powerful tool in revealing the structural packing and dynamics of lipid membranes. Using x-ray diffraction, significant information (Rand et al., 1990; Gruner, 1992) has been accumulated in recent years regarding the structural arrangements and energetics of the lipids in the planar bilayer and highly curved nonbilayer phases. Relatively little information (Cheng, 1989a–c, 1991; Chen et al., 1990a, b; Cheng et al., 1991) has been known on the molecular dynamics of the acyl chains in the nonbilayer phase, particularly within the fluorescence (nanosecond) time scale. It is believed that knowledge of both the structure and molecular dynamics of the lipids is required to better understand the intricate role of nonbilayer-preferring lipids in the function of cell membranes at the molecular level.

Several nanosecond-resolved fluorescence emission anisotropy studies (Cheng, 1989a–c; Chen et al., 1990a, 1992) aiming at understanding the intermolecular interactions among the lipids in the H_{II} phase were initiated. These studies mainly involved frequency-domain measurements of the fluorescence emission anisotropy decays of diphenylhexatriene-labeled phosphatidylcholine (DPH-PC) in several fully hydrated lipid suspensions of PE or mixtures containing PE. Using different rotational diffusion models, the value of the local orientational order parameter of DPH-PC in the lipid bilayer membranes was found to increase significantly in the presence of PE (Chen et al., 1992), implicating the presence of PE-related stress in the lipid bilayer. At present, the effects of the PE-related lateral stress on the intramolecular dynamics of the lipid acyl chains at different depths of the lipid membranes is still unclear (Cheng et al., 1991; Liu et al., 1993).

This study attempts to examine the intramolecular dynamics of the lipids in dioleoyl PE/dioleoyl PC (DOPE/DOPC) binary mixtures by the use of dipyrenyl PE lipids of different

Received for publication 24 January 1994 and in final form 18 May 1994.

Address reprint requests to Dr. Kwan-Hon Cheng, Biophysics Laboratory, Department of Physics, Box 41051, Texas Tech University, Lubbock, TX 79409-1051. Tel.: 806-742-2992; Fax: 806-742-1182; E-mail: vckhc@ttacs.ttu.edu.

0006-3495/94/08/914/08 $2.00

chain lengths that can probe the regions near the water membrane interface and bilayer center of the membranes. The DOPE/DOPC mixtures exhibit well defined composition driven bilayer-to-nonbilayer (L_α-H_{II}) phase transition behavior (Rand et al., 1990; Gawrisch et al., 1992). At low temperatures (<10°C), the binary mixtures of DOPE/DOPC are in the lamellar L_α phase at all PE contents. However, at higher temperatures (>10°), the binary mixtures enter the H_{II} phase as the PE content is increased (Rand et al., 1990; Cheng, 1991). Using the data analysis method outlined in the companion paper, the intramolecular aggregation and rotational mobility of the dipyrenyl lipids of different chain lengths are estimated at different DOPE/DOPC lipid compositions and temperatures. These intramolecular dynamics parameters allow us to examine the differential effects of PE-related lateral stress at different regions of a well defined PE/PC membrane system.

MATERIALS AND METHODS

Sample preparation

DOPE and DOPC in chloroform were purchased from Avanti Polar Lipids (Birmingham, AL) and used without further purification. No detectable fluorescence signal was found in all the lipid samples. Py_nPE and $Dipy_nPE$ were prepared from the corresponding phosphatidylcholine derivatives by phospholipase D mediated transphosphatidylation (Comfurius et al., 1976) and purified by high performance liquid chromatography on a silica column (Vauhkonen et al., 1990). The preparation of DOPE/DOPC lipid suspensions was identical to that of DMPC/cholesterol mixtures described in the companion paper.

Steady-state fluorescence spectral and nanosecond-resolved frequency-domain fluorescence intensity decay measurements

All steady-state spectral measurements were performed on either a GREG-200 fluorometer (ISS Inc., Champaign, IL) or a fast (millisecond-resolved) home-built diode array fluorometer. Either a Liconix 4240NB cw He-Cd laser (Santa Clara, CA) with an output of 10 mW at 325 nm or a 1000 W Xenon Arc Lamp with the excitation wavelength selected by a monochromator at 325 nm was employed as the excitation source. The procedures of acquiring corrected fluorescence emission spectra using the two fluorometers have been outlined in the preceding paper. Frequency-domain fluorescence intensity decay measurements of mono-chain-labeled Py_nPE and dual-chain-labeled $Dipy_nPE$ in DOPE/DOPC mixtures were performed on a GREG-200 multifrequency cross-correlation fluorometer (ISS Inc., Champaign, IL) using a Liconix 4240NB cw He-Cd laser (Santa Clara, CA) with an output of 10 mW at 325 nm as the excitation source. The operational principle of this fluorometer has been described in detail elsewhere (Lakowicz, 1983; Gratton et al., 1984) and briefly outlined in the companion paper.

Data analysis

Calculations of the kinetic parameters, (K_{dm}, K_{md}, and K_d) and (K_{da}, K_{ad}, K_{am}, K_{ma}, and K_d), of $Dipy_nPE$ from the frequency-domain fluorescence intensity decay data at 392 and 475 nm by the use of 2- and 3-state kinetic models, respectively, have been described in the companion paper. The calculation of K_m of Py_nPE from the frequency-domain fluorescence intensity decay data at 392 nm was also described in the companion paper.

RESULTS

Steady-state fluorescence spectral measurements of $Dipy_4PE$ and $Dipy_{10}PE$ in DOPE/DOPC binary lipid mixtures

Corrected steady-state fluorescence spectra were measured for $Dipy_4PE$ and $Dipy_{10}PE$ in DOPE/DOPC binary lipid mixtures of different compositions (0–100% DOPE) and at different temperatures (0–30°C). The molar ratio of the dipyrenyl lipids was fixed at 0.1%. From the fluorescence spectra, the values of the steady-state excimer-to-monomer intensity (E/M) ratio, i.e., intensity at 475 nm divided by that at 392 nm, were calculated. The data represented averages of results from at least three different sample preparations. The SEs were usually less than 10% for all samples.

Fig. 1 shows the variation of E/M ratio of $Dipy_4PE$ (*A*) and $Dipy_{10}PE$ (*B*) as a function of DOPE% and at different temperatures. In general, the values of E/M ratio for $Dipy_4PE$ were higher than those for $Dipy_{10}PE$ in DOPE/DOPC lipid membranes at identical lipid compositions and temperatures in agreement with the results obtained previously from the corresponding PC derivatives (Eklund et al., 1992). At 1°C, the E/M ratios for both $Dipy_4PE$ and $Dipy_{10}PE$ were found

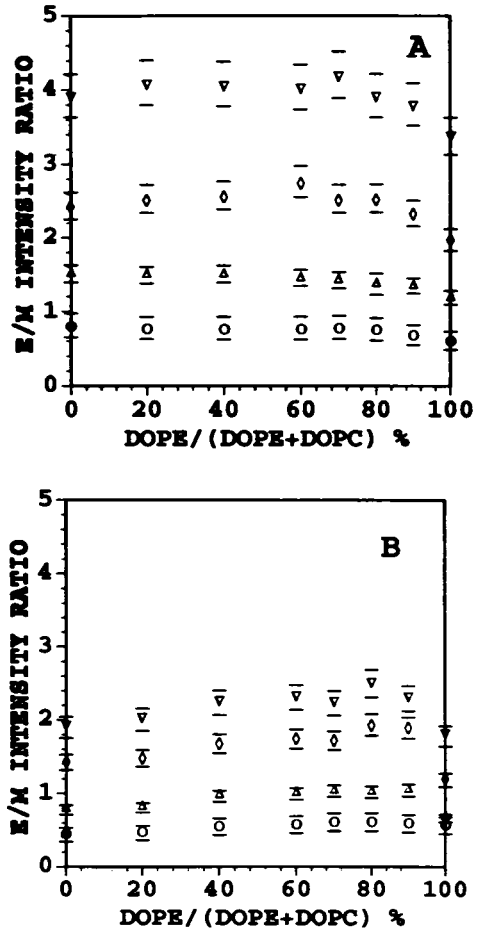

FIGURE 1 Plots of steady-state fluorescence excimer-to-monomer (E/M) intensity ratio of $Dipy_4PE$ (*A*) and $Dipy_{10}PE$ (*B*) in fully hydrated DOPE/DOPC binary mixtures as a function of DOPE content at 1°C (○), 10°C (△), 20°C (◇), and 30°C (▽). The bars indicate SEM from different samples.

to be insensitive to the DOPE% content of the lipid membranes. At 10°C, a decline in the E/M ratio was detected at 90% DOPE for both $Dipy_4PE$ and $Dipy_{10}PE$. At even higher temperatures, i.e., 20 and 30°C, the transition appeared to shift to lower DOPE% at ~80% DOPE. Using a simple titration method (Cheng et al., 1991), the E/M ratios of $Dipy_nPE$ in all DOPE/DOPC mixtures were found to be insensitive to the relative concentrations of the probes within the range of 0.01–0.5 mol% (results not shown). This observation indicated that the fluorescence properties reported in this study were mainly intramolecular events.

Measurements of the kinetic parameters of $Dipy_4PE$ and $Dipy_{10}PE$ in DOPE/DOPC binary lipid mixtures

Phase delays and demodulations of the fluorescence emissions of Py_nPE at 392 nm, and $Dipy_nPE$ at 392 and 475 nm were obtained in DOPE/DOPC binary lipid mixtures (0, 40, 80, and 100% DOPE; and at 1 and 27°C) as a function of modulation frequency. Typical plots of the frequency-domain data in the complex space are presented in Fig. 5 of the preceding paper.

Calculations of the kinetic parameters of $Dipy_4PE$ and $Dipy_{10}PE$ in DOPE/DOPC binary lipid mixtures

Both 2- and 3-state (confined and free) fits to the frequency domain data have been performed. Table 1 shows the typical values of the fitted parameters, (K_{dm}, K_{md}, and K_d) from the 2-state model; and (K_{da}, K_{ad}, K_{am}, K_{ma}, and K_d) from the 3-state model, for $Dipy_{10}PE$ in 40% DOPE mixtures at 27°C. Fitted parameters from the confined 3-state fits, i.e., (K_{da}, K_{ad}, K_{am}, and K_{ma}) and (K_{da}, K_{am}, and K_{ma}), are also shown. Similar to the results of $Dipy_{10}PC$ in DMPC membranes as shown in the companion paper, a significant improvement in the chi square of the 3-state fit over that of the 2-state fit was found. In this case, the confidence limits of the fitted parameters from the confined fits were narrower than those from the free fit. No significant improvement in the chi squares of all the confined fits was observed when compared with that of the free fit.

Similar to the results of $Dipy_nPC$ in DMPC membranes, the fitting parameters calculated from the 2-state and confined 3-state fits all converged properly. However, some of the fitting parameters calculated from the free 3-state fits with five parameters, i.e., (K_{ad}, K_{ad}, K_{am}, K_{ma}, and K_d), were not unique, particularly for $Dipy_4PE$ at most temperatures and $Dipy_{10}PE$ at low temperatures. Because of the intrinsic identifiability problem in some conditions, fitting parameters obtained from the confined 3-state fits were compared among different samples.

The fitting parameters for the 2-state model were (K_{dm}, K_{md}, and K_d), whereas those for the 3-state model were (K_{da}, K_{am}, and K_{ma}). Here K_{dm} (K_{da}) and K_{md} represent the association and dissociation rate constants of the excited dimer, respectively, and K_{am} and K_{ma} the association and dissociation rate constants of the aggregated state, respectively. The values of K_m were determined separately from the fluorescence lifetimes of Py_nPE in the identical DOPE/DOPC mixtures. Similar to Py_nPC, the values of K_m of Py_nPE were found to increase slightly from 0.7 to $1.0 \times 10^7\ s^{-1}$ with temperature from 1 to 30°C, and were insensitive to the DOPE content of the binary mixtures. Both K_m and E/M were required in the fittings. In general, significant improvements in the chi square values of the 3-state fits over those of the 2-state fits were observed for $Dipy_{10}PE$ at 27°C, whereas no significant improvements were found for $Dipy_4PE$ at 1 and 27°C, and for $Dipy_{10}PE$ at 1°C. Table 2 shows the typical fitting results obtained from the 2- and 3-state fits for $Dipy_4PE$ and $Dipy_{10}PE$ in 40% DOPE at 1 and 27°C. The confidence levels of all of the calculated parameters are also presented.

Fig. 2 shows the calculated values of K_{dm} with confidence levels for both $Dipy_4PE$ and $Dipy_{10}PE$ in DOPE/DOPC of different compositions at 1°C (*A*) and 27°C (*B*). At low

TABLE 1 Comparisons of the fitting parameters (K_{dm}, K_{md}, K_d) and (K_{da}, K_{ad}, K_{am}, K_{ma}, K_d) from the 2- and 3-state fits, respectively, for $Dipy_{10}PE$ in DOPE/DOPC binary lipid mixtures (40% DOPE) at 27°C

Fitting parameters	2-State kinetic model	3-State kinetic model		
K_{da} or K_{dm} ($10^7\ s^{-1}$)	8.63 (7.85, 9.49)	13.8 (10.2, 22.8)	15.1 (12.1, 19.8)	19.4 (16.6, 22.3)
K_{ad} or K_{md} ($10^7\ s^{-1}$)	1.43 (1.22, 1.67)	1.66 (1.15, 2.72)	1.70 (1.30, 2.62)	1.43
K_{am} ($10^7\ s^{-1}$)		3.68 (3.35, 4.35)	3.58 (3.30, 4.15)	3.80 (3.28, 4.56)
K_{ma} ($10^7\ s^{-1}$)		2.19 (1.53, 3.68)	2.20 (1.56, 3.39)	1.57 (1.48, 1.70)
K_d ($10^7\ s^{-1}$)	1.99 (1.62, 2.28)	1.89 (1.50, 2.32)	1.99	1.99
χ^2	0.42	0.18	0.19	0.19
K_{am}/K_{ma}		1.68 (0.91, 2.84)	1.63 (0.97, 2.66)	2.42 (1.93, 3.08)

Values in parentheses are confidence limits, whereas those without parentheses are fixed during the fits. The chi square (χ^2) of each fit is also shown.

TABLE 2 Kinetic parameters, (K_{dm}, K_{md}, K_d) and (K_{da}, K_{ma}, K_{md}), of $Dipy_4PE$ and $Dipy_{10}PE$ in DOPE/DOPC binary mixtures (40% DOPE) obtained from 2- and 3-state fits, respectively

Sample	K_{dm} (10^7 s^{-1})	K_{md} (10^7 s^{-1})	K_d (10^7 s^{-1})	K_{da} (10^7 s^{-1})	K_{ma}/K_{md}	$\chi_3^2(\chi_2^2)$
$Dipy_4PE$	6.95	1.86	1.61	12.3	3.76	
(1°C)	(6.13, 7.97)	(0.89, 2.95)	(1.03, 1.09)	(9.92, 14.5)	(1.90, 11.9)	2.36 (2.93)
$Dipy_{10}PE$	5.4	3.01	0.92	10.5	4.26	
(1°C)	(4.41, 6.54)	(2.64, 3.38)	(0.80, 1.30)	(9.07, 12.0)	(3.06, 10.6)	1.20 (1.53)
$Dipy_4PE$	12.2	0.78	1.69	13.0	5.28	
(27°C)	(10.1, 14.2)	(0.68, 0.89)	(1.58, 1.78)	(11.8, 14.6)	(3.06, 10.6)	0.28 (0.37)
$Dipy_{10}PE$	8.63	1.43	1.99	19.4	2.42	
(27°C)	(7.85, 9.49)	(1.22, 1.67)	(16.2, 2.28)	(16.6, 22.3)	(1.93, 3.08)	0.17* (0.42)

Values in parentheses are confidence limits. The chi squares of the 3- and 2-state fits are given by χ_3^2 and χ_2^2, respectively.
* Significant improvement in the 3-state fit over the 2-state fit ($p < 0.05$).

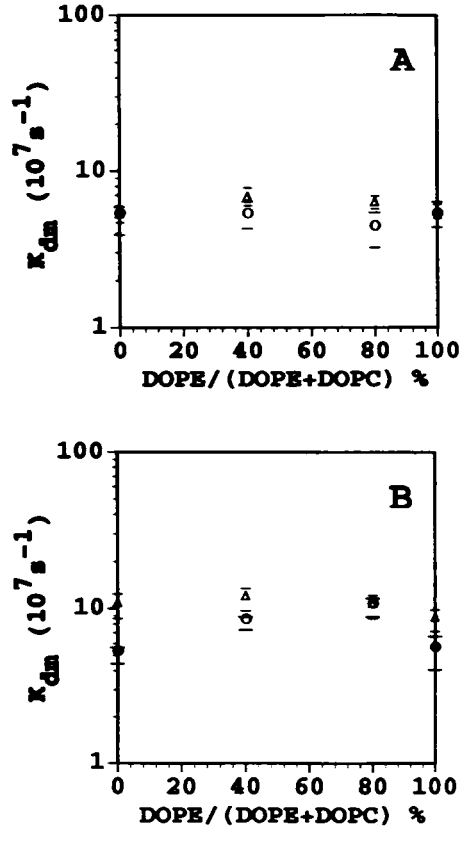

FIGURE 2 Plots of K_{dm} of $Dipy_4PE$ (△) and $Dipy_{10}PE$ (○) in DOPE/DOPC binary mixtures as a function of DOPE content at 1°C (*A*) and 27°C (*B*). The parameter K_{dm} was calculated based on the 2-state kinetic model. The bars indicate the confidence levels of the fitted parameters.

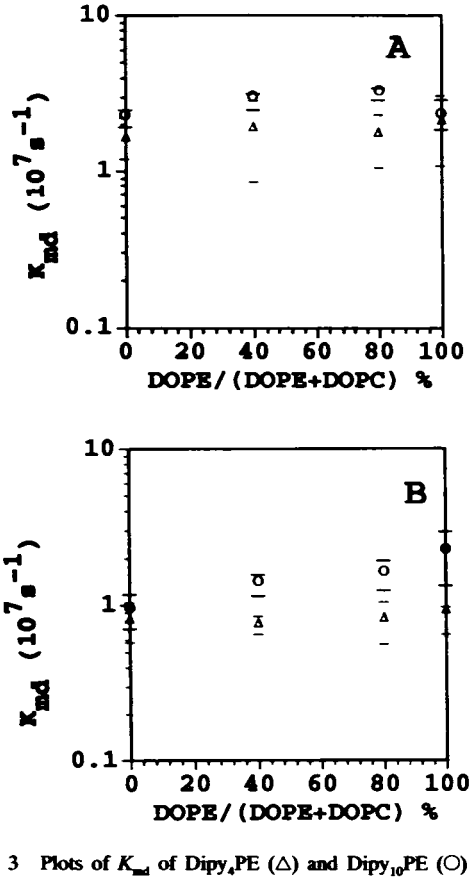

FIGURE 3 Plots of K_{md} of $Dipy_4PE$ (△) and $Dipy_{10}PE$ (○) in DOPE/DOPC binary mixtures as a function of DOPE content at 1°C (*A*) and 27°C (*B*). The parameter K_{md} was calculated based on the 2-state kinetic model. The bars indicate the confidence levels of the fitted parameters.

temperature (1°C), the values of K_{dm} for both $Dipy_4PE$ and $Dipy_{10}PE$ were around 5–8 × 10^7 s^{-1} and were insensitive to the DOPE% of the membranes. At higher temperature (27°C), the values of K_{dm} for $Dipy_4PE$ increased to around 10 × 10^7 s^{-1} but were still insensitive to DOPE%. At the same high temperature, the K_{dm} of $Dipy_{10}PE$ increased twofold, i.e., ~5 to 10 × 10^7 s^{-1}, as the DOPE% increased from 0 to 80% DOPE, and declined back to ~5 × 10^7 s^{-1} as the DOPE content reached 100% DOPE. Figs. 3 and 4 show the calculated values of K_{md} and K_d for both $Dipy_4PE$ and $Dipy_{10}PE$ at 1 (*A*) and 27°C (*B*). The values of K_{md} were found to be in the range of 1–3 × 10^7 s^{-1}, whereas those of K_d were found to be in the range of 1–2 × 10^7 s^{-1} for both $Dipy_4PE$ and $Dipy_{10}PE$. These values were quite independent of the composition of the membranes at either low or high temperature. Those values of K_{md} and K_d were used as fixed K_{md} and K_d parameters in the confined 3-state fit.

Figs. 5 and 6 show the calculated values of K_{da} (*A*) and K_{ma}/K_{md} (*B*) for $Dipy_4PE$ and $Dipy_{10}PE$ at 1 and 27°C, respectively. At 1°C, the values of K_{da} for $Dipy_{10}PE$ at 80 and

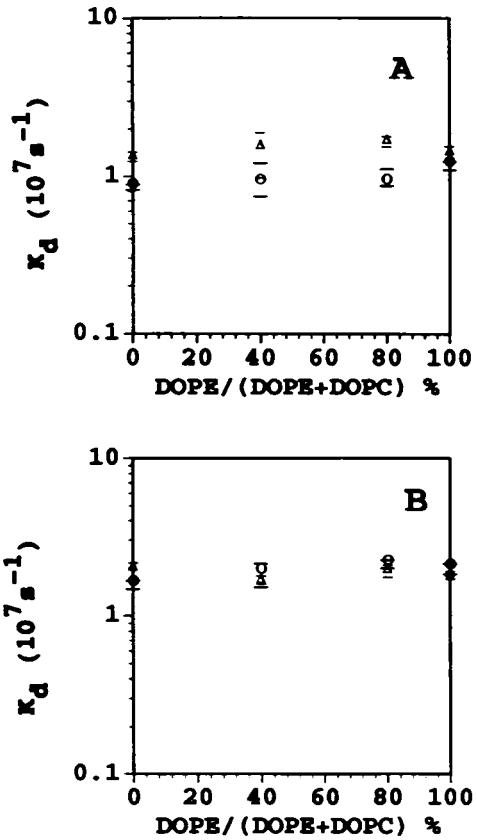

FIGURE 4 Plots of K_d of $Dipy_4PE$ (△) and $Dipy_{10}PE$ (○) in DOPE/DOPC binary mixtures as a function of DOPE content at 1°C (*A*) and 27°C (*B*). The parameter K_d was calculated based on the 2-state kinetic model. The bars indicate the confidence levels of the fitted parameters.

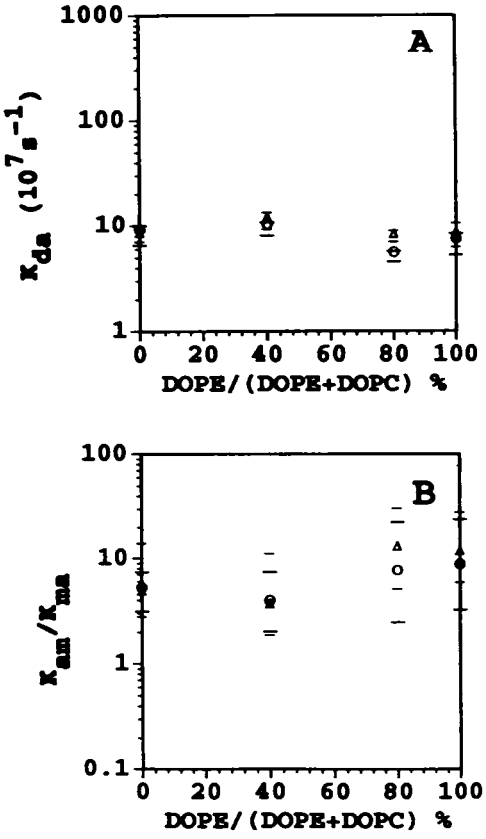

FIGURE 5 Plots of K_{da} (*A*) and K_{am}/K_{ma} (*B*) of $Dipy_4PE$ (△) and $Dipy_{10}PE$ (○) in DOPE/DOPC binary mixtures as a function of DOPE content at 1°C. The parameters K_{da} and K_{am}/K_{ma} were calculated based on the 3-state kinetic model. The bars indicate the confidence levels of the fitted parameters.

100% DOPE were around 8×10^7 s^{-1} and slightly lower than those at 0 and 40%, whereas the values of K_{da} for $Dipy_4PE$ were similar to those for $Dipy_{10}PE$ and showed very little dependence on DOPE%. At the same low temperature, the values of K_{am}/K_{ma} for $Dipy_4PE$ and $Dipy_{10}PE$ were in the range of 5–10 and were also insensitive to DOPE%. It was observed that the confidence intervals for K_{am}/K_{ma} were larger than those of K_{da}. At 27°C (Fig. 6), the values of K_{da} and K_{am}/K_{ma} for $Dipy_4PE$ were around 10×10^7 s^{-1} and 1–5, respectively, and remained insensitive to DOPE%. However, for $Dipy_{10}PE$ and the same high temperature, the values of K_{da} started at 50×10^7 s^{-1} and decreased almost twofold, whereas those of K_{am}/K_{ma} started at 0.9 and increased more than threefold, as the DOPE content increased from 0 to 80%. Thereafter, the value of K_{da} increased fivefold and that of K_{am}/K_{ma} decreased sixfold as the DOPE content finally reached 100%. It was also observed that the values of K_{da} of $Dipy_4PE$ were always lower than those of $Dipy_{10}PE$ at all DOPE%.

DISCUSSION

Frequency-domain fluorescence intensity decay measurements on $Dipy_4PE$ and $Dipy_{10}PE$ in binary lipid mixtures of DOPE/DOPC have been performed at different temperatures (1 and 27°C) and lipid compositions (0, 40, 80, and 100% DOPE). Using the 3-state kinetic model, the rotational mobility and extent of aggregation of the intralipid pyrenes, in terms of K_{da} and K_{am}/K_{ma}, respectively, at the regions near the bilayer center (long chain $Dipy_{10}PE$) and the water/membrane interface (short-chain $Dipy_4PE$) have been estimated.

At low temperature (1°C), the binary lipid mixtures are known to be in the bilayer form (Rand et al., 1990; Gawrisch et al., 1992; Cheng, 1991). In this case, the values of K_{da} and K_{am}/K_{ma} obtained from the 3-state model, as well as those of K_{da} from the 2-state model, are insensitive to the PE content of the membranes for both $Dipy_4PE$ and $Dipy_{10}PE$. These results indicate that the acyl chains are in the condensed or closely packed state at low temperature, and that their internal motions are independent of the structure of the lipid headgroups. Moreover, lacks of significant improvements in the 3-state fits over the 2-state fits, as well as the nonuniqueness of the free 3-state fits, are found. These results might indicate that the acyl chains are already quite close to each other so that a 1-step process, $A^* \rightleftharpoons D^*$ (Birks et al., 1963; Sugar, 1991; Cheng et al., 1991; Sassaroli et al., 1993; Liu et al., 1993), is already sufficient to describe the excited-state reaction (see Fig. 2 in the companion paper) of the short- and long chain intralipid pyrene moieties in the lipid membranes at low temperature.

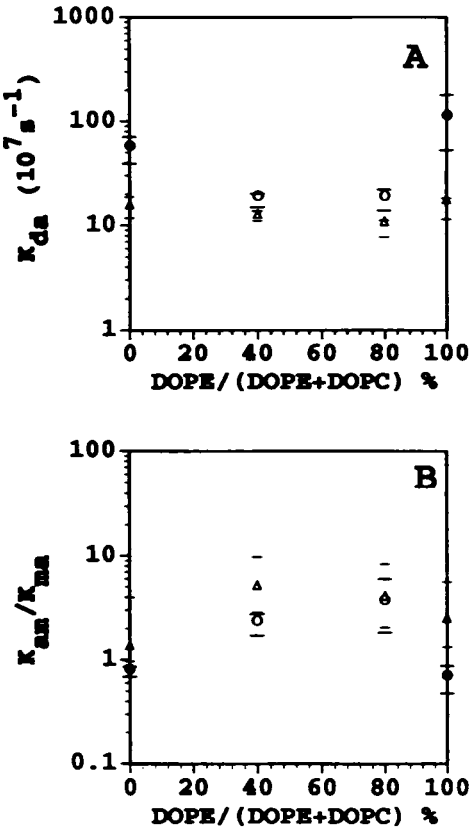

FIGURE 6 Plots of K_{da} (*A*) and K_{am}/K_{ma} (*B*) of $Dipy_4PE$ (△) and $Dipy_{10}PE$ (○) in DOPE/DOPC binary mixtures as a function of DOPE content at 27°C. The parameters K_{da} and K_{am}/K_{ma} were calculated based on the 3-state kinetic model. The bars indicate the confidence levels of the fitted parameters.

At high temperature (27°C), the binary mixtures are known to be in the bilayer form at 0–80% DOPE (Cheng, 1991). For $Dipy_{10}PE$, the values of K_{da} and K_{dm} decrease, whereas those of K_{am}/K_{ma} increase, progressively with PE%. These results suggest that the internal rotation and flexing of the acyl chains become more hindered and the intramolecular chain aggregation increases as the PE content of the bilayer membranes increases. These PE-associated increases in the hinderance of mobility and aggregation for $Dipy_{10}PE$, therefore, reflect the increase of lateral stress in the presence of PE (Rand et al., 1990; Seddon, 1990; Chen et al., 1992). In addition, as the PE% increases further to 100%, the hinderance in the mobility decreases and a concomitant decrease in the aggregation occurs, indicating that the "stressed" lipid layer can be relaxed once the lipids adopt the inverted hexagonal phase. Interestingly, no similar changes were found for $Dipy_4PE$. Our results, therefore, provide indirect evidence that the PE-associated stress effects the intramolecular dynamics of the lipid membranes more at the region near the bilayer center than that near the water/membranes interface where the acyl chains always remain in a closely packed state. Furthermore, the intramolecular rotational rates for $Dipy_4PE$ are quite insensitive to the DOPE% at all temperatures and are lower than those for $Dipy_{10}PE$ at high temperature. This again supports the notion that the mobility of the chains near the water/membranes interface is more hindered than that near the center of the bilayer (De Loof et al., 1991; Rey et al., 1992; Kodati and Lafleur, 1992; Pearce and Harvey, 1993; Alam, 1993) even at high temperature. Note that the K_{da} and K_{am}/K_{ma} from the 3-state model, as well as the K_{dm} from the 2-state model, for $Dipy_{10}PE$ in the inverted hexagonal phase (100% PE) are very similar to those in the bilayer phase (0% PE) at the same temperature (27°C). This indicates that most of the PE-associated stress can be relieved when the lipids adopt the inverted hexagonal phase.

Because PE is a major lipid component in most animal cell membranes, the detection of PE-related enhancement in the intramolecular aggregation of the acyl chains near the bilayer center might have some biological implications. This PE-induced increase in intramolecular aggregation can play an important role in several membrane-related phenomena, e.g, protein-mediate active ion transport (Cheng and Hui, 1986; Cheng et al., 1986) and protein kinase C activity (Slater et al., 1994) and fusion (Siegal, 1986). Of course, the other roles of PE on the hydration of the membrane surface (Hui, 1993) and the creation of transient or metastable packing defects (Siegal, 1986) at the domain boundaries of the membranes cannot be ignored.

The description of the intralipid conformation of the acyl chains in terms of K_{am}/K_{ma} is more straightforward as compared with the effective concentration factor as described in a previous study (Liu et al. 1993). Here, only K_{da} is required to describe the intralipid dynamics, whereas K_{da} and f (transition rate of the pyrene from one lattice point to another) were used by Liu et al. (1993) based on a modified 2-dimensional lattice model (Sugar et al., 1991b). It is important to note that the number of fitted parameters is between three and five in this study as compared with five in Liu et al. (1993), and all the calculations have been performed in the complex space using an independently acquired steady-state fluorescence parameter, E/M ratio, to weight the two linked fittings at 392 and 475 nm frequency domain data (see companion paper and Sugar et al., 1991a, b). These fitting procedures in the complex space provide a much faster convergence and further ensure the identifiability (Davenport et al., 1986; Ameloot et al., 1986) of the calculated parameters in the fittings than do those carried out in the real space (Liu et al., 1993).

The current 3-state model assumes the existence of the ground and excited intermediate states, i.e., A and A^*, respectively. According to the reaction scheme as shown in Fig. 2 of the companion paper, a direct excitation of the A into the A^* is possible. Thus, other than the $M^* \rightarrow A^* \rightarrow D^*$ pathway, a dimer state D^* can also be formed via the $A^* \rightarrow D^*$ pathway upon excitation of one of the two intralipid pyrene molecules in a dipyrenyl lipid. As far as we know, there are no dimers in the ground state, which would be the necessary condition of measuring excimer immediately after excitation. Note that only the close apposition of the pyrene moieties is not a sufficient condition for the immediate excimer formation (Sugar et al., 1991b). Our current 3-state model suggests that translational diffusion and reorientation (2-step

process), or reorientation (1-step process), of pyrene moieties precede the dimer formation after excitation.

A different 3-state model can also be considered. In this alternative 3-state model, there are two species for the monomer, fast and slow. Both fast and slow species can form the dimer, but there is no interconversion between these two species. The above competitive reaction scheme is obviously different from the current consecutive (monomer-aggregate-dimer) reaction scheme. This competitive scheme might represent another possible mechanism for describing the excited state reaction of intralipid pyrenes. However, it might be difficult to envision what would hinder the interconversion of these species in a lipid membrane system. For the sake of simplicity, this alternative 3-state model, as well as other excited state kinetic models, will only be examined and compared with our current 3-state model in future investigations. There are still several limitations in the current 3-state model, and detailed discussions of them are given below.

First, the use of a single rate constant K_{am} to describe the approaching rate of the excited pyrene molecule to its ground state neighbor to form an aggregated state (Sugar, 1991; Liu et al., 1993) might be an over-simplification of the actual process within the lipid molecule. This is because the segmental motions (Kodati and Lafleur, 1992; Alam, 1993) of the chains, e.g., *trans-gauche* isomerization, wobbling of the whole chain and torsional motion of the entire chain with respect to the pivotal point attached to the glycerol backbone, are actually 3-dimensional. In this respect, there is vertical displacement as well as lateral movement of the covalently attached pyrene molecules in a dipyrenyl lipid embedded in the host lipid matrix. The rate constant K_{am}, therefore, should represent a combination of those different motions, and does not provide any information of the individual contributions of the different processes (Rey et al., 1992) within the context of this current 3-state reaction model.

Second, the association and dissociation rate constants for the ground aggregated state, K_{am} and K_{ma}, respectively, are assumed to be identical to those for the excited aggregated state (see Fig. 2 in the companion paper). This assumption still awaits to be justified.

Finally, the values of K_{md} and K_d obtained from the 2-state fits are used to fix the values of K_{ad} and K_d in the confined 3-state fits. As discussed in this and the companion papers, the confined fits ensure proper convergence of the recovered parameters in some conditions: $Dipy_4PE$ or PC at all temperatures, and $Dipy_{10}PE$ or PC at low temperatures. Yet the confinements of those parameters cannot be strictly justified based on mathematical argument alone. It is worthwhile to mention, however, that both K_{ad} and K_{md} refer to the same rate constant, dissociation rate of dimer, of intralipid pyrene derivatives in the membranes. Similar to the photodecay parameters K_m, K_d, and K_{fd}/K_{fm}, we speculate without direct proof that this dimer dissociation rate constant should depend more on the photophysical property of the pyrene dimer itself rather than on the physical state of the host lipid membranes. Based on the unconfined or free 3-state fit parameters for $Dipy_{10}PE$ in DOPE/DOPC and $Dipy_{10}PC$ in DMPC/cholesterol mixtures, the K_{ad} and K_d are found to be relatively insensitive to the lipid composition than the other rate constants, K_{da}, K_{am}, and K_{ma}. Furthermore, the recovered values of K_{ad} and K_d from the free 3-state fits are very similar to those of K_{md} and K_d from the 2-state fits.

In conclusion, with the above assumptions and limitations of the kinetic models in mind, the reported intramolecular dynamics parameters K_{da} and K_{am}/K_{ma} allow us to estimate separately the rotational mobility and state of aggregation of the acyl chains at defined regions of the membranes in response to the PE-related stress as shown in this paper, as well as to the phase properties and effect of cholesterol as shown in the companion paper. Moreover, the values of the recovered parameter K_{dm} from the 2-state fits also provide similar, although less detailed, intramolecular dynamics information about the physical state of the two binary DOPE/DOPC and DMPC/cholesterol membranes. Because most of the previous quantitative fluorescence investigations on lipid layer dynamics were focused on the reorientational order and lateral mobility of the whole lipid molecule, the availability of the intralipid molecular dynamics parameters can provide a new dimension in exploring the behavior of lipids and site-specific lipophilic molecules in the membranes within the nanosecond time scale. Whether the intramolecular dynamics parameters, K_{dm}, K_{da}, and K_{am}/K_{ma}, can be used to detect and characterize bilayer packing defects and domains in model and biological membranes is still unknown, and is actively being investigated in our laboratories.

We would like to thank one of the reviewers for suggesting the use of competitive excited state reaction scheme to study the intramolecular excimer kinetics of dipyrenyl lipids.

This work was supported by the Robert A. Welch Research Foundation (D-1158) and National Institutes of Health grant CA47610 given to K. H. Cheng, and the Finnish Academy given to P. Somerharju.

REFERENCES

Alam, T. M. 1993. Molecular dynamics in lipid bilayers. Anisotropic diffusion in an odd restoring potential. *Biophys. J.* 64:1681–1690.

Ameloot, M., J. M. Beechem, and L. Brand. 1986. Compartmental modeling of excited-state reactions: identifiability of the rate constants from fluorescence decay surfaces. *Chem. Phys. Lett.* 129:211–219.

Birks, J. B., D. J. Dyson, and I. H. Munro. 1963. "Excimer" fluorescence II. Lifetime studies of pyrene solutions. *Proc. R. Soc. Lond.* 275:575–588.

Chen, S.-Y., K. H. Cheng, B. W. Van Der Meer, and J. M. Beechem. 1990a. Effects of lateral diffusion on the fluorescence anisotropy in hexagonal lipid phase II. An experimental study. *Biophys. J.* 58:1527–1537.

Chen, S.-Y., K. H. Cheng, and D. M. Ortalano. 1990b. Lateral diffusion study of excimer forming lipids in lamellar to inverted hexagonal phase transition of unsaturated phosphatidylethanolamine. *Chem. Phys. Lipids.* 53:321–330.

Chen, S.-Y., K. H. Cheng, and B. W. Van Der Meer. 1992. Quantitation of lateral stress in lipid layer containing nonbilayer phase preferring lipids by frequency-domain fluorescence spectroscopy. *Biochemistry.* 31: 3759–3768.

Cheng, K. H. 1989a. Fluorescence depolarization study of lamellar liquid crystalline to inverted cylindrical micellar phase transition of phosphatidylethanolamine. *Biophys. J.* 55:1025–1031.

Cheng, K. H. 1989b. Fluorescence depolarization study on non-bilayer phases of phosphatidylethanolamine and phosphatidylcholine lipid mixtures. *Chem. Phys. Lipids.* 51:137–145.

Cheng, K. H. 1989c. Time-resolved fluorescence depolarization study of lamellar to inverted cylindrical micellar phase. *Proc. SPIE Int. Soc. Opt. Eng.* 1054:160–167.

Cheng, K. H. 1991. Infrared study of the polymorphic phase behavior of dioleoylphosphatidylethanolamine and dioleoylphosphatidyl- choline. *Chem. Phys. Lipids.* 60:119–125.

Cheng, K. H., S.-Y. Chen, P. Butko, B. W. Van Der Meer, and P. Somerharju. 1991. Intramolecular excimer formation of pyrene-labeled lipids in lamellar and inverted hexagonal phases of lipid mixtures containing unsaturated phosphatidylethanolamine. *Biophys. Chem.* 39:137–144.

Cheng, K. H., and S. W. Hui. 1986. Correlation between the bilayer stabilization and activity enhancement by diacylglycerols in reconstituted Ca-ATPase vesicles. *Arch. Biochem. Biophys.* 244:382–386.

Cheng, K. H., J. R. Lepock, S. W. Hui, and P. L. Yeagle. 1986. The role of cholesterol in the activity of reconstituted Ca-ATPase vesicles containing unsaturated phosphatidylethanolamine. *J. Biol. Chem.* 261: 5081–5087.

Comfurius, P., E. M. Bevers, and R. F. A. Zwaal. 1976. Enzymatic synthesis of phosphatidylserine on small scale by use of one-phase system. *J. Lipid Res.* 31:1719–1721.

Davenport, L., J. R. Knutson, and L. Brand. 1986. Excited-state proton transfer of equilenin and dihydroequilenin: interaction with bilayer vesicles. *Biochemistry.* 25:1186–1195.

De Loof, H., S. C. Harvey, J. P. Segrest, and R. W. Pastor. 1991. Mean field stochastic boundary molecular dynamics simulation of a phospholipid in a membrane. *Biochemistry.* 30:2099–2113.

Eklund, K. K., J. A. Virtanen, P. K. J. Kinnunen, J. Kasurinen, and P. J. Somerharju. 1992. Conformation of phosphatidylcholine in neat and cholesterol containing crystalline bilayers. Application of a novel method. *Biochemistry.* 31:8560–8565.

Epand, R. M., and R. F. Epand. 1994. Calorimetric detection of curvature strain in phospholipid bilayers. *Biophys. J.* 66:1450–1456.

Gawrisch, K., V. A. Parsegian, D. A. Hajduk, M. W. Tate, S. M. Gruner, N. L. Fuller, and R. P. Rand. 1992. Energetics of a hexagonal-lamellar-hexagonal phase transition sequence in dioleoylphosphatidylethanolamine membranes. *Biochemistry.* 31:2856–2864.

Gratton, E., D. M. Jameson, and R. D. Hall. 1984. Multifrequency phase and modulation fluorometry. *Annu. Rev. Biophys. Bioeng.* 13:105–124.

Gruner, S. M. 1992. Nonbilayer lipid phases. *In* The Structure of Biological Membranes. P. Yeagle, editor. CRC Press, Boca Raton, FL. 211–250.

Hui, S. W. 1993. Lipid molecular shape and high curvature structures. *Biophys. J.* 65:1361–1362.

Keller, S. L., S. M. Bezrukov, S. M. Gruner, M. W. Tate., I. Vodyanoy, and V. A. Parsegian. 1993. Probability of alamethicin conductance states varies with nonlamellar tendency of bilayer phospholipids. *Biophys. J.* 65: 23–27.

Kodati, V. R., and M. Lafleur. 1992. Comparison between orientational and conformational orders in fluid lipid bilayers. *Biophys. J.* 64:163–170.

Lakowicz, J. R. 1983. Principle of Fluorescence Spectroscopy. Plenum Press, New York. 126 pp.

Lewis, N. A. H., R. N. McElhaney, P. E. Harper, D. C. Turner, and S. M. Gruner. 1994. Studies of the thermotropic phase behavior of phosphatidylcholines containing 2-alkyl substituted fatty acyl chains: a new class of phosphatidylcholines forming inverted nonlamellar phases. *Biophys. J.* 66:1088–1103.

Liu, L., K. H. Cheng, and Somerharju. 1993. Frequency-resolved intramolecular excimer fluorescence study of lipid bilayer and non-bilayer phases. *Biophys. J.* 64:1869–1877.

Pearce, L. L., and S. C. Harvey. 1993. Langevin dynamics studies of unsaturated phospholipids in a membrane environment. *Biophys. J.* 65:1084–1092.

Rand, R. P., N. L. Fuller, S. M. Gruner, and V. A. Parsegian. 1990. Membrane curvature, lipid segregation, and structural transitions for phospholipids under dual-solvent stress. *Biochemistry.* 29:76–87.

Rey, A., A. Kolinski, J. Skolnick, and Y. K. Levine. 1992. Effect of double bonds on the dynamics of hydrocarbon chains. *J. Chem. Phys.* 92: 1240–1249.

Sassaroli, M., M. Vauhkonen, P. Somerharju, and S. Scarlata. 1993. Diphenylphosphatidylcholines as membrane fluidity probe. Pressure and temperature dependence of the intramolecular rate. *Biophys. J.* 64: 137–149.

Seddon, J. M. 1990. Structure of the inverted hexagonal (H_{II}) phase, and non-lamellar transitions of lipids. *Biochim. Biophys. Acta.* 1031:1–69.

Siegel, D. P. 1986. Inverted micellar intermediates and the transitions between lamellar, cubic and inverted hexagonal phases. II. Implications for membrane-membrane interactions and membrane fusion. *Biophys. J.* 49: 1171–1183.

Slater, S. J., F. J. Taddeo, and C. Ho. 1994. The modulation of protein kinase C activity by membrane lipid bilayer structure. *J. Biol. Chem.* 269: 4866–4871.

Sugar, I. P. 1991. Use of fourier transforms in the analysis of fluorescence data. 1. A general method for finding explicit relationships between photophysical models and fluorescence parameters. *J. Phys. Chem.* 95: 7508–7515.

Sugar, I. P., J. Zeng, M. Vauhkonen, P. Somerharju, and P. L.-G. Chong. 1991a. Use of fourier transforms in the analysis of fluorescence data. 2. Fluorescence of pyrene-labeled phosphatidylcholine in lipid bilayer membrane. Test of the Birks model. *J. Phys. Chem.* 95:7516–7523.

Sugar, I. P., J. Zeng, and P. L.-G. Chong. 1991b. Use of fourier transforms in the analysis of fluorescence data. 3. Fluorescence of pyrene-labeled phosphatidylcholine in lipid bilayer membrane. A three-state model. *J. Phys. Chem.* 95:7524–7534.

Vauhkonen, M., M. Sassaroli, P. Somerharju, and J. Eisinger. 1990. Dipyrenylphosphatidylcholines as membrane fluidity probes. Relationship between intramolecular and intermolecular excimer formation rates. *Biophys. J.* 57:291–300.